Electrical Engineering (2024) 106:3129–3142
https://doi.org/10.1007/s00202-023-02092-y

ORIGINAL PAPER

Modeling, analysis, and shielding of the electric field between extra-high-voltage AC transmission lines and oil pipelines

Montaser Abdelsattar[1] · Hamdy A. Ziedan[2] · Ahmed Elnozahy[2]

Received: 25 July 2023 / Accepted: 13 October 2023 / Published online: 5 December 2023

Abstract
The static charges and induced voltages from extra-high-voltage alternating current transmission lines (EHVACTLs) on parallel oil pipelines (POPLs) raise the risk levels for people and animals. Thus, the objective of this paper was to reduce and/or mitigate the electric field which is concentrated on POPLs by using grounded shield wires under EHVACTLs. Three techniques are employed to reduce the electric field effects on POPLs of two distinct types of transmission lines (TLs), 500 kV and 220 kV. The first technique involves raising the tower's height to improve the clearance space between the POPLs and the TL conductors. The second technique is increasing the horizontal distance between the POPLs and the nearest stressed conductors of the TL. The third technique involves placing shield wires beneath the stressed conductors of the EHVACTLs. The electric field under the EHVACTLs is calculated with and without the grounded shield wires using charge simulation method. The results of the first technique revealed that with increasing the tower height from 10 m to 15, 20, 25, and 30 m, the electric field decreased by 43.75%, 62.5%, 68.75%, and 75%, respectively. Herein, employing the second technique, the electric field intensity is reduced by 20% and 21% depending on the POPL placed at a distance from the right stressed conductor equal to the horizontal clearance between conductors of 500 kV and 220 kV, respectively. Besides, the results of the third technique proved that the shield wires under the EHVACTLs reduced the electric field intensity on the POPLs by 17.65% and 24.71% for 500-kV and 220-kV TLs, respectively.

Keywords EHVACTLs · Electric field · Height of towers · Mathematical modeling · Mitigation · Parallel oil pipelines · Shield wires

Abbreviations

AC	Alternating current
CP	Cathodic protection
CSM	Charge simulation method
DC	Direct current
EM	Electromagnetic
EMF	Electromagnetic field
EHVACTLs	Extra-high-voltage alternating current transmission lines
ESD	Electrostatic discharge
HVPL	High-voltage power lines
POPLs	Parallel oil pipelines
PSO	Particle swarm optimization
TLs	Transmission lines
UHVDC	Ultra-high-voltage direct current

✉ Montaser Abdelsattar
Montaser.A.Elsattar@eng.svu.edu.eg

✉ Hamdy A. Ziedan
ziedan@aun.edu.eg

Ahmed Elnozahy
ahmed.alnozahy@aun.edu.eg

[1] Electrical Engineering Department, Faculty of Engineering, South Valley University, Qena 83523, Egypt

[2] Department of Electrical Engineering, Faculty of Engineering, Assiut University, Assiut 71516, Egypt

1 Introduction

The transfer of electrical power from generation stations to consumers' locations is a complicated process due to the various factors that control it. One of these factors, the TLs should be close to/parallel to main roads for easy construction/building or maintenance. Also, the transmission process of the oil in pipelines should be close to/parallel to the main

roads for the same purposes. Therefore, the combinations of TLs and oil pipelines may be parallel to each other and on the same roads for long distances. There is a concentration of static charges and induced voltages on POPLs due to the high values of the electric fields from the TLs. These static charges and the induced voltages have high values that are very harmful to humans and animals in case the POPLs are not well grounded.

One of the most significant sources of the magnetic field is the high-voltage transmission lines. Electromagnetic field (EMF) interaction with buried pipes has been of considerable concern to literature in recent years. EMF intrusion on pipelines situated in utility corridors is a true and significant issue that can threaten both the operator's protection and the pipeline's quality. Pipelines are susceptible to being installed in electric utility corridors comprising high-voltage AC transmission lines. When there is a long-term induced AC voltage on a pipeline, contacting the pipeline or appurtenances may be unsafe and even life-threatening for operations staff. AC discharge can also result in pipe corrosion. Shwehdi et al. [1] estimated the deposition of the AC voltages due to high-voltage transmission lines on buried pipelines in the Eastern region of Saudi Arabia. The basic methods, instructions, required details, and cautions for carrying out such estimations were presented. The results showed that the EMI evaluation accuracy required sufficient soil resistance at each section of the pipeline. Also, the resistance of pipelines coating significantly affected the accuracy.

Abdel-Salam and Ziedan [2] introduced the assessment of the inductive and capacitive induced voltages on a gas pipeline that existed under the AC transmission line. Boundary points on the surface of phase conductors and the pipeline where the boundary conditions are met were chosen to determine the values of the simulation charges. The induced voltages were estimated for pipelines located in the air underneath 500-, 380-, and 66-kV power lines and in the ground underneath 220-kV lines. The results showed that the inductive induced voltage is low compared with the capacitive one. The capacitive induced voltage on the pipeline is situated in the air underneath the transmission line, while the inductive induced voltage is located on the ground under the transmission line.

Abdel-Salam et al. employed a charge simulation-based technique to calculate the induced voltages on fence wire/pipeline underneath a high-voltage transmission line [3–5]. The technique was based on the methodology of charge simulation and considered the disruptions of the electrical field and the induced voltage due to the existence of the fence wire/pipeline below the line. The induced voltages and capacitance-to-ground and the short-circuit current-to-ground on fence wire/pipeline below 230- and 380-kV high-voltage lines were measured, correlated with the calculated values, and addressed on nearby components to AC power transmission lines in the presence of electric field induction.

Electric fields and induced voltages on oil trucks crossing the extra-high-voltage alternating current (EHVAC) transmission line of 380-kV double circuits rating 900 MVA in Saudi Arabia were mitigated by Ziedan et al. [6]. The modeling approach was based on the charge simulation method (CSM) for evaluating the electric field distribution, induced charges, and currents on the body of an oil truck. The induced emf experimental measurements were taken from an actual oil truck filled with gasoline crossing 380-kV double-circuit transmission lines. The author suggested two methods to mitigate electric fields and induced voltage on the truck's body: first, through increasing the height of towers which were positioned in the crossing area, second, under the stressed conductors, shield ground wires were utilized.

The features and impacts of ultra-high-voltage direct current (UHVDC) electromagnetic interference and geomagnetic storms on underground pipelines have been studied by Liu et al. [7–9]. Compared to the Shanghai Temple-Shandong Project's 6250 A grounding pole current conditions on January 2, 2017, and the Zalute-Qingzhou, the effect of ± 800-kV UHVDC transmission monopole service on underground oil pipelines was assessed. The effect of geomagnetic storms on the protection of underground oil pipelines was also evaluated based on geoelectric field monitoring records. The findings revealed that the effect on the pipeline of the DC grounding pole current was associated with the distance among the pipeline and ground electrode, the potentiated operating state, and the insulating flange spacing on the pipeline. The geomagnetic storm had a stronger interfering effect on submerged pipelines compared with the DC of the grounding pole.

The topic of AC corrosion remains inspiring researchers. Numerous variables that impacted the corrosion rate of underground pipelines because of the interference with overhead high-voltage TLs were studied. The processes of induced AC voltages, which are summed up as capacitive, inductive, and conductive coupling, have been investigated by many authors. Al-Gabalawy et al. [10] analyzed only the induced AC voltage on the pipelines due to inductive coupling in steady-state conditions. A holistic numerical simulation for pipelines, power lines, induced voltage mitigating devices and cathodic protection (CP) have been presented. Potassium hydroxide polarization cells were electrically represented since the most common mitigating device for discharging the induced AC voltage from the pipeline to the soil was known to be such cells. The study outcomes revealed the profiles of the induced AC voltage along the pipeline, the CP for the pipeline, the maximal voltage points, and the effect on the CP performance of the installed AC mitigation systems.

Djekidel et al. [11] proposed a technique based on the electromagnetic induction law of Faraday to determine the induced voltage produced by the high-voltage power line on a parallel aerial metal pipeline in its near area in steady-state operation condition. Besides, the process of induced voltage mitigation using the passive loop technique as paired with the algorithm of particle swarm optimization (PSO) was defined. The existence of a pipeline near an aerial power line greatly disrupted the mapping of the magnetic induction created by this power line. By improving the location of the loop conductors, increasing the number of loops, and using a magnetic shielding substance of high relative permeability, the mitigation performance was dramatically improved. The outcome of the numerical simulation was compared to the extracted outcome of Carson's formulas.

Popoli et al. [12] suggested a numerical technique for measuring currents and voltages generated by adjacent aerial power lines on underground pipelines. The suggested approach was based on the discretization of the pipeline route into multiple parallel sections of the power line. The corridor portion corresponding to each section of the pipeline was an electrical multi-port element, the electrical parameters of which were derived by a 2D finite element analysis. Consequently, the obtained components were assembled into a network embodying the entire corridor's physical characteristics. Thus, to broaden the capabilities of traditional two-dimensional field analysis, circuit analysis was used. The physical implications of the crossing between a pipeline and a power line were addressed, and a convergence analysis was implemented to examine the best method for a range of different crossing angles to be followed for pipeline subdivisions. The obtained outcomes for different crossing angles revealed that a convergence analysis should be conducted if an oblique route is discretized with a collection of parallel sections to ensure that the discretization process does not influence the obtained results, particularly when considering small crossing angles.

The corrosive impacts of electromagnetic induction, which is produced by double-circuit high-voltage power lines (HVPL) on the buried steel X70 pipelines, were diagnosed by Ouadah et al. [13]. The electromagnetic interference between the steel pipeline and the double-circuit HVPL that was described in the buried X70 steel pipeline as the propagation of the magnetic field and the induced AC densities was studied. The vertical distance between the HVPL double-circuit and the steel pipeline X70 and the conductor phase sequence orientation were all factors that contributed to the interference. Consequently, electrochemical measurements were used to describe the corrosion polarization features of X70 steel in simulated soil at different AC densities. The findings revealed that the corrosion rate of the X70 steel raised with an increase in the density of AC, implying that the induced AC density had intensified the corrosion level of the X70 steel relative to that in the non-existence of the density of the AC. The authors inferred from these observations that the electromagnetic induction induced by the HVPL of the double circuit influenced the electrochemical feature of the steel pipeline X70 and expedited the corrosion of the pipeline.

Electrostatic discharge (ESD) is a physical phenomenon that can damage electronic components via its high discharge current, which may exceed a few amps in a matter of nanoseconds. A further significant aspect of ESD is the associated high-frequency electromagnetic (EM) fields emitted by the ESD occurrence. Electronic appliances that are impacted by ESD are likewise affected by induced voltage caused by EM fields. The most prevalent strategies for computing the ESD electromagnetic fields, focusing on the optimal methods for minimizing computational effort, were examined in [14]. Furthermore, the experimental setups and measurement devices for measuring the electric and magnetic fields produced via ESD were reviewed in [14]. The authors in [14] recommended the EM field to be measured during the verification of ESD generators by specifying certain limitations. Furthermore, the EM field created by ESD generators should be taken into account by the designers of such generators during the design process.

The authors in [15] developed an ANN software tool for evaluating the electric and magnetic fields emitted by ESDs. Real input and output data obtained via enormous experimental measurements in the high-voltage laboratory at National Technical University of Athena were utilized in training, validation and testing phases. By merely recording the discharge current, this developed software tool analyzed the electromagnetic field emitted by ESDs in an easy and precise manner. The authors in [15] pointed out that the developed software tool could be highly beneficial to the laboratories doing ESD tests.

From the literature, the main contributions of this study can be summarized in the following:

1. Calculate the electric field under 500-kV and 220-kV TLs without adding the shield wires under the stressed HV wires on the level of the parallel oil pipelines.
2. Re-calculate the electric field under the 500-kV and 220-kV TLs by adding the shield wires under the stressed HV wires.
3. Study the effect of varying the height of the towers to minimize the electric field's concentration on the parallel oil pipeline level (at a height of one meter above the ground).
4. Study the effect of increasing the horizontal distance between the POPLs and the nearest stressed conductors of the TL on the concentration of the electric field.
5. Study the effect of increasing the clearance distance between the stressed HV and shield wires.

2 Research methods

In this section, the calculation of the induced voltage on the parallel oil pipelines (POPLs) based on the determination of the electric field under the extra-high-voltage AC transmission lines (EHVACTLs) will be obtained by using the well-known technique of charge simulation method (CSM) [10–16]. The technique to mitigate the concentration of electric fields in parallel oil pipelines is via installing shield wires beneath the EHVACTLs. Despite the fact that the field distribution around stressed HV conductors is non-uniform, the CSM is the most accurate approach for determining the electric field under the EHVACTLs. Schematic graphs of 500-kV and 220-kV TLs are shown in Figures 1 and 2, respectively. A 500-kV transmission line is constructed by 1-circuit, 3-phase, and 3-bundle sub-conductors per phase, as shown in Figure 1. A 220-kV transmission line is constructed from 2-circuit, 3-phase, 2-bundle sub-conductors per phase, as shown in Figure 2. It is assumed that the EHVACTLs system is in the X–Y plane and is infinity on Z-axis. The simulated surface line charges are assumed inside the conductors at radius r_f ($r_f = f \cdot r_c$) where f is a fraction from 0 to 1 (in this study, is chosen by 0.5) and r_c is the radius of sub-conductors. The number of simulated surface line charges inside each sub-conductor, grounding wire, oil pipeline, and shield wire is N_1, N_2, N_3, and N_4, respectively. The number of sub-conductors, ground wires, oil pipelines, and shield wires is assumed n_c, n_g, n_p, and n_{sh}, respectively. Thus, the total number of the unknown simulated surface line charges is [16–18]:

$$n = (N_1 \times n_c) + \left(N_2 \times n_g\right) + \left(N_3 \times n_p\right) + (N_4 \times n_{sh}) \quad (1)$$

Other sets of boundary points are used to satisfy the boundary conditions, equal to the applied voltage on the sub-conductors and zero on the grounding wires, the oil pipelines, and the shield wires. The total number of boundary points equals the total number of undefined charges $Q_{s,j}$.

At any boundary point at coordinates (x_i, y_i), the potential ϕ_i is a function of the potential coefficient P_{ij} and the potential due to all surface line charges at (x_j, y_j) which is expressed as follows [19–21]:

$$\varnothing_i = \sum_{j=1}^{n} P_{ij} Q_{s,j} \quad (2)$$

$$P_{ij} = \ln\left(\frac{1}{R_1 R_2 R_3 R_4}\right);\ i = 1,\ 2,\ 3,\ \ldots,\ n;\ j = 1,\ 2,\ 3,\ \cdots,\ n \quad (3)$$

where

$$R_1^2 = \left(x_i - x_j\right)^2 + \left(y_i - y_j\right)^2;$$
$$R_2^2 = \left(x_i + x_j\right)^2 + \left(y_i - y_j\right)^2;$$
$$R_3^2 = \left(x_i + x_j\right)^2 + \left(y_i + y_j\right)^2;$$
$$R_4^2 = \left(x_i - x_j\right)^2 + \left(y_i + y_j\right)^2;$$

A matrix equation will be formulated when applying the boundary conditions for the formula of Eqn. (2) expressed as follows [20, 21]:

$$[P][Q_s] = [V_b] \quad (4)$$

where $[P]$ is the $n \times n$ matrix of potential coefficient; $[Q_s]$ unknown simulation charges matrix with dimension $n \times 1$; and $[V_b]$ boundary points potential values matrix with dimension $n \times 1$.

To determine the unknown surface line charges Q_s, the matrix formula of Eq. (4) should be solved first. The accuracy of the solution is checked by choosing checkpoints that are located in between the boundary points. After the accuracy of the solution is checked, the electric field ξ is calculated under the EHVACTLs.

$$\xi_x = \left(\frac{\delta}{2\pi\varepsilon_o}\right)\sum_{j=1}^{n} Q_{sj}\left(\left(x_p - x_j\right)\left(\frac{1}{R_1^2} + \frac{1}{R_4^2}\right) + \left(x_p + x_j\right)\left(\frac{1}{R_2^2} + \frac{1}{R_3^2}\right)\right) \quad (5)$$

$$\xi_y = \left(\frac{\delta}{2\pi\varepsilon_o}\right)\sum_{j=1}^{n} Q_{sj}\left(\left(y_p - y_j\right)\left(\frac{1}{R_1^2} + \frac{1}{R_4^2}\right) + \left(y_p + y_j\right)\left(\frac{1}{R_2^2} + \frac{1}{R_3^2}\right)\right) \quad (6)$$

$$\xi = \sqrt{\left(\xi_x^2 + \xi_y^2\right)} \quad (7)$$

The magnetic field density B in Tesla, which is a function of phase current I, is found as follows [2]:

$$B = \frac{\mu_0 H_1 I}{2\pi R}\left[\frac{3R^2 + H_1^2}{R^4 - 2R^2 H_1^2 \cos(2\varnothing_r) + H_1^4}\right] \quad (8)$$

where R is the distance from any point of interest and the center phase conductor, H_1 magnetic field, which is measured in amperes per meter (A/m), μ_0 the free space magnetic permeability, and ϕ_r the angle between the vector R and the horizontal line passing the phase conductors.

The inductive induced voltage V_{emf} on the body oil pipelines is determined as follows:

$$V_{emf} = \omega I Z_m \tag{9}$$

where ω is the radian frequency, I the current, and Z_m the mutual impedance between oil pipelines and phase conductors of the transmission line, which carry an AC obtained using Carson's formula [5, 24, 25].

3 Results and discussion

The previous methodology is applied for two kinds of TLs, the first one is the 500-kV transmission line, as shown in Figure 1, and the second one is the 220-kV transmission line, as shown in Figure 2. There is an oil pipeline in parallel with the TLs. The oil pipelines are at the height of one meter over the ground with a diameter of 1 m. The distance between the oil pipelines and the nearest phase of the line Do is a parameter of the field calculation. The calculation is done for both 500- and 220-kV transmission lines to mitigate the effect of electric field concentration on the parallel oil pipelines by increasing the height of the towers, increasing the horizontal distance between the POPLs and the nearest stressed conductors of the TL, and to add shield wires under the stressed phases of the EHVTLs.

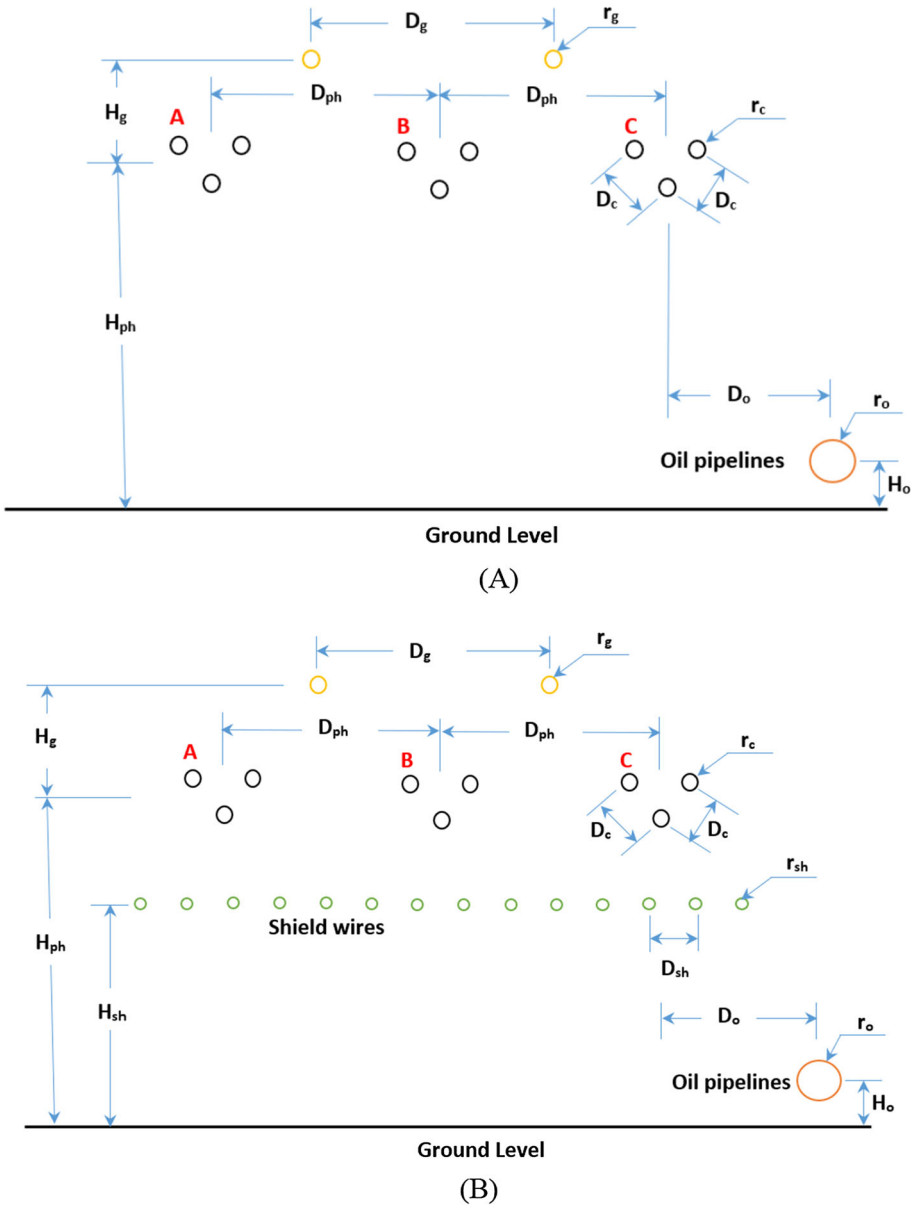

Fig. 1 Configuration of 500-kV TL: **A** without shield wires and (**B**) with shield wires

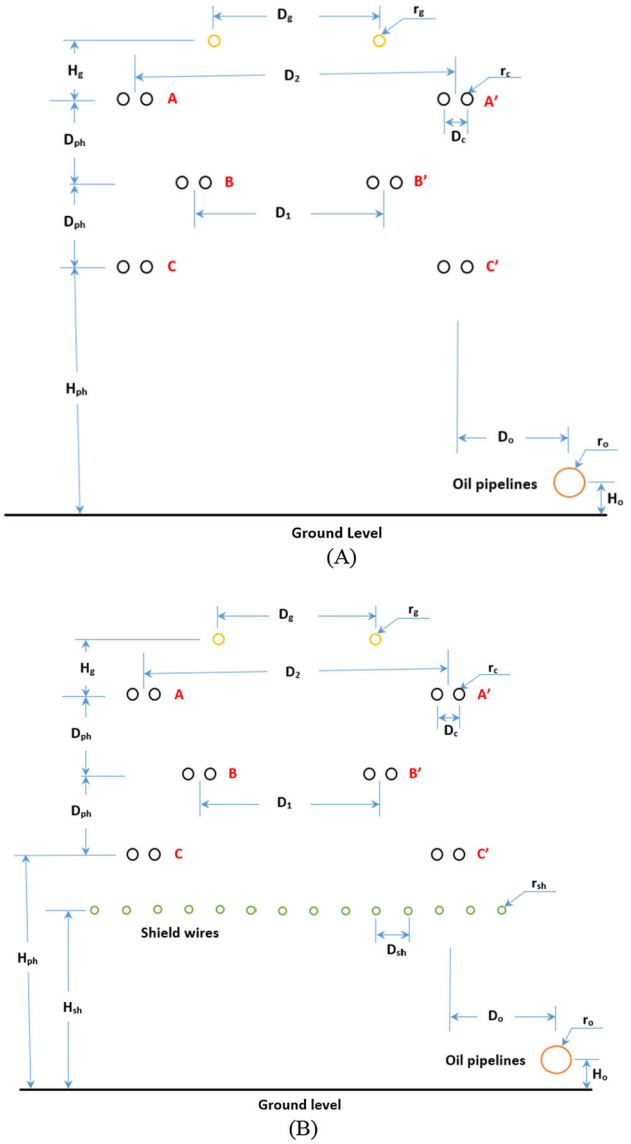

Fig. 2 Configuration of 220-kV TL: **A** without shield wires and (**B**) with shield wires

3.1 Results of 500-kV EHVACTLs with parallel oil pipelines

A 500-kV EHVACTL with parallel oil pipelines without shield wires is shown in Figure 1A, and the shield wires under the stressed EHVACTLs are shown in Figure 1B. There are 1 circuit, 3 sub-conductors (bundle) per phase with radius r_c of 0.0153 m, the distance between the sub-conductors D_c is adjusting to 0.5 m, the clearance between the stressed conductors (phases) D_{ph} is 12 m, and the height of the stressed conductors over the ground level H is a variable in this study (10, 15, 20, 25, and 30 m). Two grounding conductors with wire radius r_g, a function of the sub-conductor radius r_c ($r_g = 0.5 \times r_c$), and with a height H_g of 9 m above the stressed wires, and spacing between each other D_g of 18 m.

For the parallel oil pipelines, the radius r_o is 0.5 m, the height above the ground H_o is 1 m, and the clearance between the oil pipelines and the nearest stressed conductor (phase) D_o is a function of clearance between the stressed conductors (phases) D_{ph} in this study as shown in Figure 1A.

In the shield wires with wire radius r_{sh}, which is a function of the sub-conductor radius r_c ($r_{sh} = 0.5 \times r_c$) with an adjustment of wire spacing D_{sh} of 1 m, the total number of shield wires is 31, and the height above the ground level H_{sh} is a function of the conductors (phases) height H, which varies in this study (75%, 50%, and 25%) as shown in Figure 1B. Shield wires are grounded, meaning that the applied voltage on them equals zero.

The CSM is employed to determine the electric field under the stressed lines and its concentration on the parallel oil pipelines. The number of line charges inside the sub-conductor, shield wires, and the oil pipeline is chosen as 16, 6, and 6, respectively. All these line charges are located inside the sub-conductor, shield lines, and the oil pipeline at a radius of its half main radius. The accuracy of the CSM is about 2.7×10^{-10}% on the stressed HV conductors and about 7.13×10^{-11}% on shield wires and the oil pipelines. The accuracy of CSM is calculated mathematically, and the accuracy is the difference between the calculated induced voltage due to simulated charges and the applied voltages on stressed wires and grounded oil pipelines over the applied (stressed) voltage [16, 17].

Figure 3 shows the electric field calculation at a height of one meter over the ground, which is the same level as the parallel oil pipelines under the 500-kV EHVACTLs without using shield wires. The x-axis presents the horizontal distance under the 1 circuit, 3 sub-conductors per phase of 500-kV TL. The center point of x-axis (at $x = 0$) is aligned with the middle phase (phase B) of 500-kV TL. The positive x-axis is at the right of phase B, while the negative x-axis is at the left of phase B. The values of the electric field are a function of the height of the stressed wires H or the height of the tower. The electric field decreases with increasing the height of the tower at the level of a parallel oil pipeline, as shown in Figure 3. The distribution of the electric field under the three phases of the 500-kV TL should be uniform, but it is not uniform because of parallel oil pipelines, which increases the concentration of the electric field under the nearest stressed conductor (phase), as shown in Figure 3. The electric field is decreased with increasing the height of the tower, as shown in Figure 3. With increasing the tower height from 10 m to 15, 20, 25, and 30 m, the electric field decreased by 43.75%, 62.5%, 68.75%, and 75%, respectively, as shown in Figure 3A.

When the position of the POPL is exactly under the right phase of the TL, as shown in Figure 3A, the concentration of the electric field on the POPL is increased than other phases

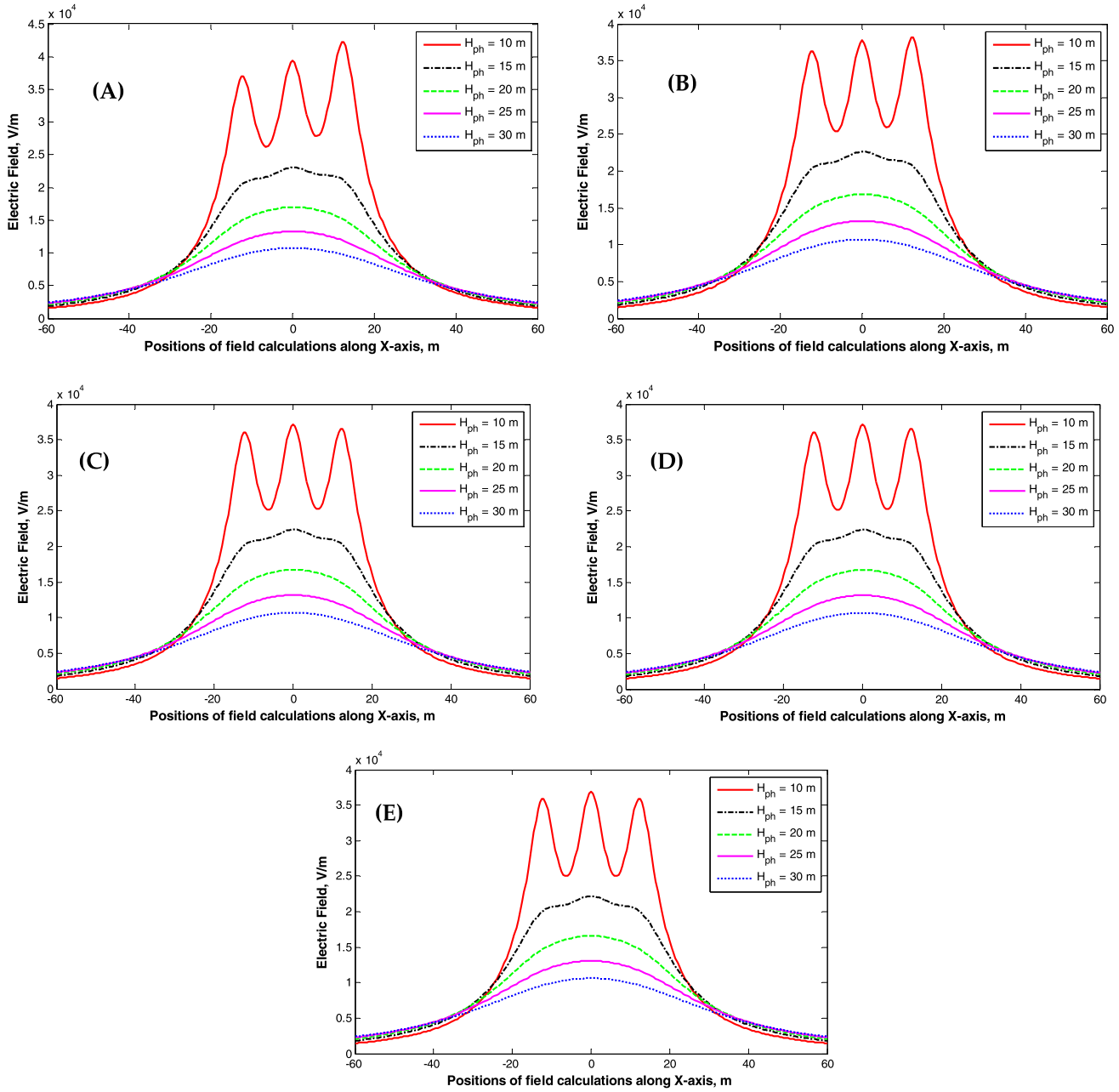

Fig. 3 Calculation of the electric field at a height of one meter over the ground at the same parallel oil pipelines level under the 500-kV EHVACTLs without using shield wires with the position of the parallel oil pipelines is: **A** exactly under the right phase of the TL, **B** at 0.5 × Dph from the right phase of the TL, **C** at 1.0 × Dph from the right phase of the TL, **D** at 2.0 × Dph from the right phase of the TL, and (**E**) at 4.0 × Dph from the right phase of the TL

(conductors) of the 500-kV TL. With increasing the distance between the parallel oil pipelines and the nearest conductor (0.5, 1.0, 2.0 and 4.0 × D_{ph}), the electric field distribution is decreased, and its shape is more uniform at the level of parallel oil pipelines, as shown in Figure 3B, C, D, and E, respectively.

Figure 4 shows the electric field under the 500-kV EHVACTLs using shield wires which is decreased from 3.5 × 10^4 V/m when the POPL is exactly under the right phase of the TL with height of phase (H_{ph}) at 10 m above the ground level to 2 × 10^4, 1.5 × 10^4, 1.0 × 10^4, and 0.75 × 10^4 V/m with H_{ph} at 15, 20, 25, and 30 m, respectively. Figure 4 shows the results of the electric field calculation at the height of one meter over the ground with considering the shield wires under the stressed wires (under the 500-kV EHVACTLs) at the height of 75% of the tower height H. In

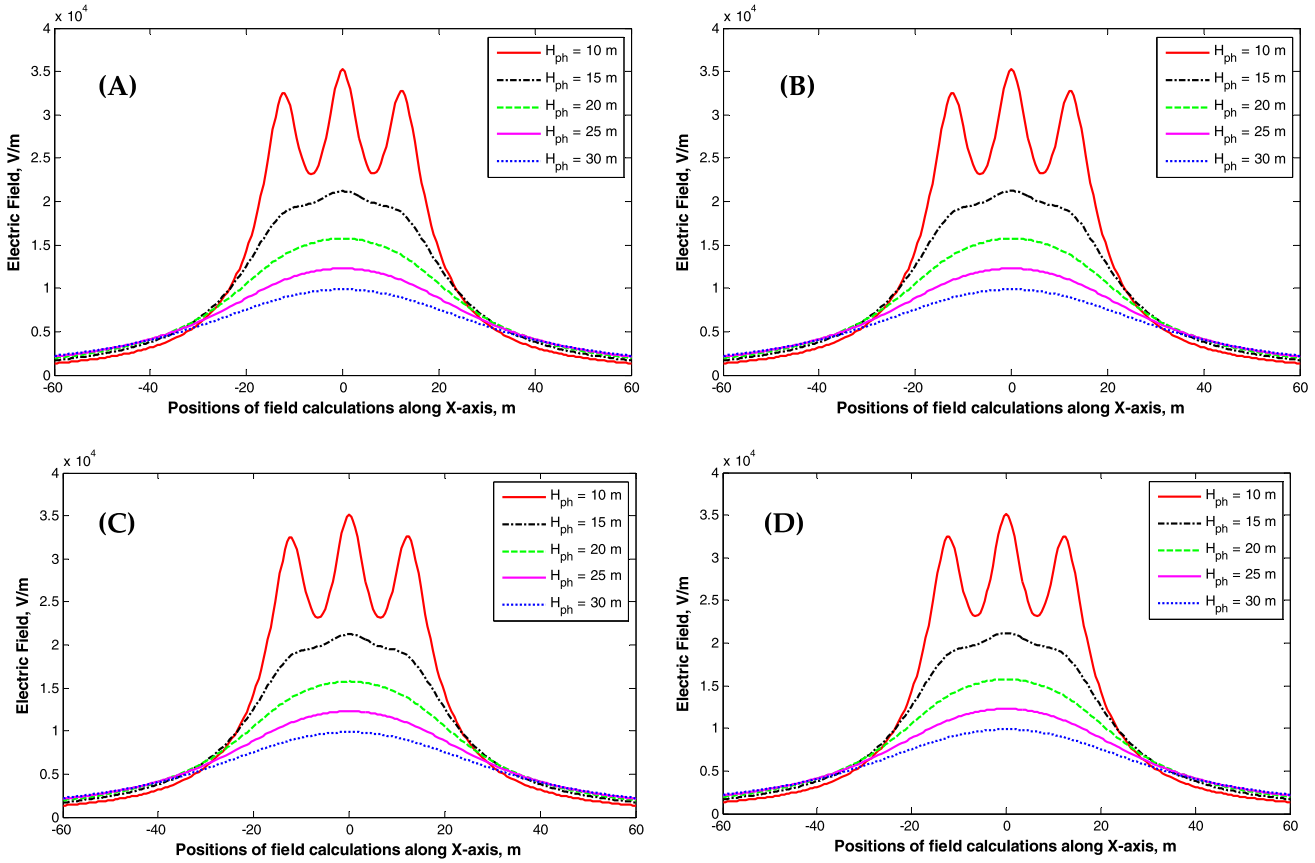

Fig. 4 Calculation of the electric field at the height of one meter over the ground at the same parallel oil pipelines level under the 500-kV EHVACTLs using the shield wires at the height of 75% of the tower height H with the position of the parallel oil pipelines is: **A** exactly under the right phase of the TL, **B** at 1.0 × Dph from the right phase of the TL, **C** at 2.0 × Dph from the right phase of the TL, and (**D**) at 4.0 × Dph from the right phase of the TL

the case of height 10 m, the ground shieling wires will be at 2.5 m below of stressed wires and at 7.5 m (75% of height) above the ground level, not the opposite.

Figure 5 shows the results of the electric field calculation using the shield wires at the level of oil pipelines (at the height of one meter over the ground) under the 500-kV EHVACTLs with the position of the POPL at 2.0 × D_{ph} from the right phase of the TL at the height of 75%, 50%, and 25 % of the tower height H. It is worth noting that the height of shield wires and the position of POPLs are 75% of the tower height and 2.0 × D_{ph} from the right phase of the TL, respectively, for both Figures 4C and 5A. Consequently, the electric field concentration and distribution are the same as depicted in Figures 4C and 5A.

3.2 Discussion of results at a 500-kV EHVACTLs with parallel oil pipelines

It is clear from Fig. 3A though E that with increasing the height of towers, the concentration of the electric field on the oil pipelines level over the ground is decreased. Also, the shape of electric field is more uniformly with the increasing the position of the oil pipelines from the phases (conductors) of EHVAC towers.

With increasing horizontal distance between POPL and the conductors of EHVAC, the concentration of the electric field on oil pipelines is decreased underneath of EHVACTLs stressed by 500 kV as depicted in Fig. 3. The concentration of the electric field is decreased from 4.25 × 10^4 V/m when the POPL is exactly under the right phase of the TL with height of phase (H_{ph}) at 10 m above the ground level to 3.8 × 10^4, 3.6 × 10^4, 3.5 × 10^4, and 3.4 × 10^4 V/m for the position of the POPL at 0.5 × Dph, 1.0 × Dph, 2.0 × Dph, and 4.0 × Dph from the right phase, respectively. This corresponds to 10.6, 15.3, 17.6, and 20% reduction in electric field concentration at positions of 0.5 × Dph, 1.0 × Dph, 2.0 × Dph and 4.0 × Dph for the POPL at the right phase, respectively. Thus, the electric field concentration is mitigated at the same point underneath the EHVACTLs due to shifting the POPLs away

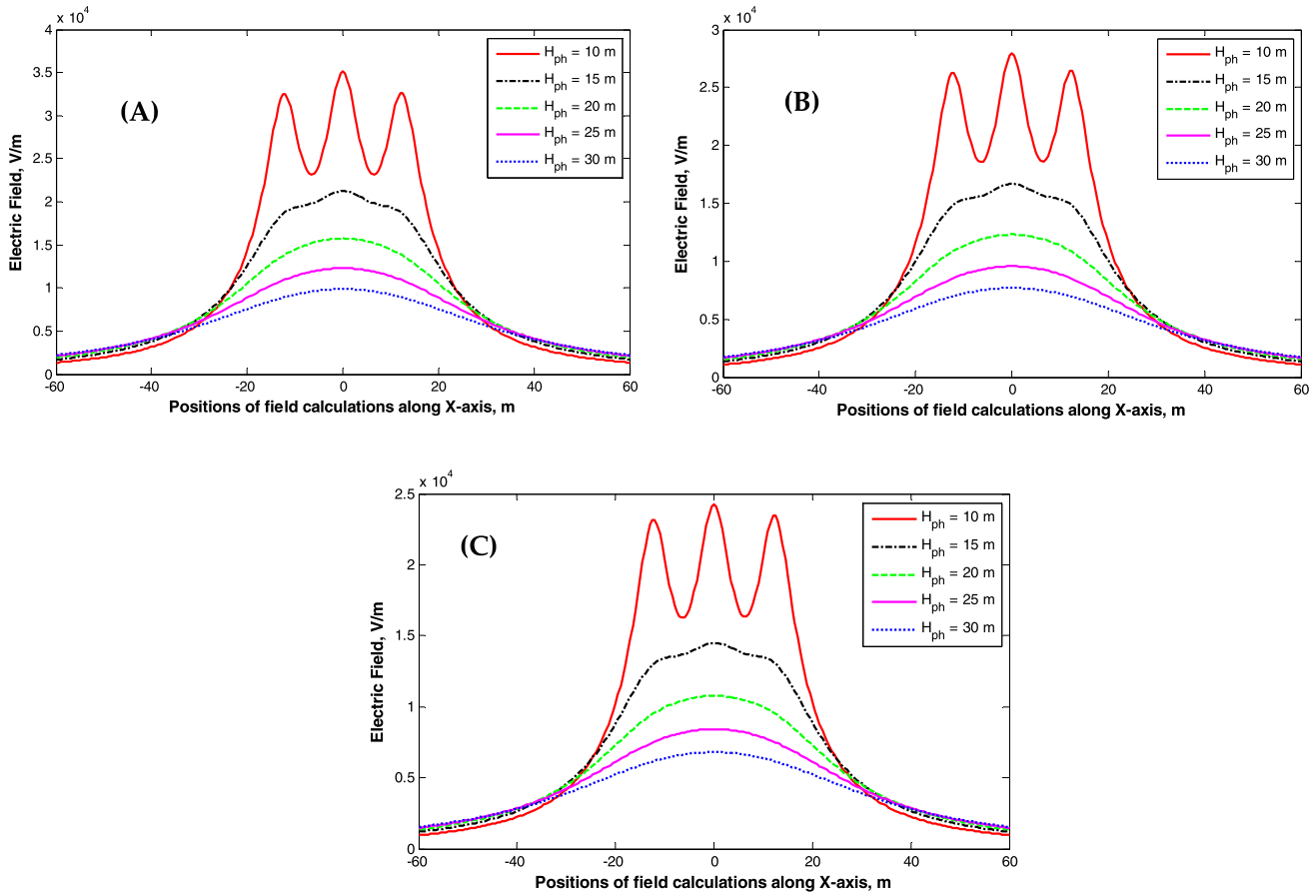

Fig. 5 Calculation of the electric field at the height of one meter over the ground at the same parallel oil pipelines level under the 500-kV EHVACTLs with using the shield wires with the position of the parallel oil pipelines is at 2.0 × Dph from the right phase of the TL at the height of: **A** 75% of the tower height H, **B** 50% of the tower height H, and **C** 25% of the tower height H

to different distances in the right of x-axes which approve the effect of POPLs position on the electric field concentration.

It is quite clear that using the shield wires under the 500-kV EHVACTLs reduces the concentration of the electric field at the oil pipelines surface, and the shape is more uniform if the position of the POPL is exactly under the right phase of the TL or at 1.0, 2.0, and 4.0 × Dph from the right phase of the TL as illustrated in Fig. 4A, B, C, and D, respectively. The electric field concentration under the EHVACTLs and on the surface of the parallel oil pipelines is affected by the shield wires.

With comparison between Figs. 3A through E and 4A through E, the concentration of the electric field on oil pipelines using shield wires under the EHVAC conductors is reduced to suitable values and did not affect by the position of the oil pipelines under or near the EHVAC conductors as in shown in A through E. The electric field concentration is mitigated from 3.75×10^4 V/m without using shield wires to 3.5×10^4 after using the shield wires. This corresponds to a 6.7% reduction in field concentration as depicted in Figs. 3 and 5, respectively. This concludes that the shield wires protect the POPL from the effect of electric field concentration as well as make it possible to keep the POPL everywhere under the stressed EHVAC conductors.

The significant effect of distance between the ground shield wires and the stresses wires is addressed in Fig. 5A, B, and C. With increasing the distance between the ground shield wires and the stressed wires via changing the height of the shield wires (H_{sh}), the electric field on the level of oil pipelines is decreased, as shown in Fig. 5A, B, and C, respectively. The concentration of the electric field at the shield wires (H_{sh}) height 75%, 50%, and 25% of the tower height is decreased to 3.6×10^4, 2.8×10^4, and 2.4×10^4 V/m with height of phase (H_{ph}) at 10 m above the ground level as depicted in Fig. 5A, B, and C, respectively. This corresponds to 17.2, 35.6, and 44.8% reduction on electric field concentration as compared by the value of electric field without shield wires ($= 4.35 \times 10^4$ V/m).

3.3 Results of 220-kV EHVACTLs with parallel oil pipelines

A 220-kV EHVACTL with parallel oil pipelines without shield wires is shown in Figure 2A, and the shield wires under the stressed EHVACTLs are shown in Figure 2B. There are 2 circuits, 2 sub-conductors per phase with radius r_c of 0.0135 m, the distance between the sub-conductors D_c is adjusting to 0.3 m, the clearance (height) between the stressed conductors (phases) D_{ph} in the same circuit is 9.2 m, and the clearance between the same phases in the two circuits D_1 and D_2 is 9 m and 17.1 m, respectively. The height of the lowest stressed conductors over the ground level H is a variable in this study (10, 15, 20, 25, and 30 m). There are two grounding conductors with wire radius r_g, which is a function of the sub-conductor radius r_c ($r_g = 0.5 \times r_c$) and with height H_g of 9 m above the highest stressed conductors, and with spacing between each other D_g of 15 m.

For the parallel oil pipelines, the radius r_o is 0.5 m, the height above the ground H_o is 1 m, and the clearance between the oil pipelines and the nearest stressed conductor (phase) D_o is a function of clearance between the stressed conductors (phases) D_{ph} in this study as shown in Figure 2.

In the shield wires with wire radius $r_{sh,}$ which is a function of the sub-conductor radius r_c ($r_{sh} = 0.5 \times r_c$) with an adjustment of wire spacing D_{sh} of 1 m, the total number of shield wires is 31, and the height above the ground level H_{sh} is a function of the conductors (phases) height H in this study (75%, 50%, and 25%) as shown in Figure 2B. Herein, the shield wires are grounded, meaning the applied voltage on them equals zero.

The CSM is employed to determine the electric field under the stressed lines and its concentration on the parallel oil pipelines. The number of line charges inside the sub-conductor, shield wires, and the oil pipeline is chosen as 16, 6, and 6, respectively. All these line charges are located inside the sub-conductor, shield lines, and the oil pipeline at a radius of its half main radius. The accuracy of the CSM is about 8.13×10^{-10} % on the stressed HV conductors and about 1.5×10^{-10} % on shield wires and the oil pipelines. The accuracy of CSM is calculated mathematically, and the accuracy is the difference between the calculated induced voltage due to simulated charges and the applied voltages on stressed wires and grounded oil pipelines over the applied (stressed) voltage [16, 17].

Figure 6 shows the electric field calculation at the height of one meter over the ground, which is the same level as the parallel oil pipelines under the 220-kV EHVACTLs without using shield wires. The x-axis is presenting the horizontal distance under the 2 circuits, 2 sub-conductors per phase, 220-kV TL. The center point of x-axis (at $x = 0$) is aligned with the middle point between the 2 circuits. The right circuit (A', B', and C') is aligned with the positive x-axis, while the left circuit (A, B and C) is aligned with the negative x-axis. The values of the electric field are a function of the height of tower H. The electric field diminishes with increasing the height of the tower at the level of a parallel oil pipeline, as shown in Figure 6. Again, the electric field distribution is not uniform because oil pipelines increase the concentration of the electric field under the nearest stressed conductor (phase). When the position of the parallel oil pipeline is exactly under the right phase of the TL, as shown in Figure 6A, the concentration of the electric field on the oil pipelines is increased than other phases (conductors) of the 220-kV TL. With an increase in the distance between the parallel oil pipelines and the nearest conductor (1.0, 2.0, and 4.0 × Dph), the electric field distribution is decreased, and its shape is more uniform at the level of parallel oil pipelines, as shown in Figure 6B, C, and D, respectively.

With increasing horizontal distance between POPL and the conductors of EHVAC, the concentration of the electric field on oil pipelines is decreased at 220 kV, as shown in Figure 6. The concentration of the electric field is decreased from 1.7×10^4 V/m when the POPL is exactly under the right phase of the TL with height of phase (H_{ph}) at 10 m above the ground level to 1.6×10^4, 1.55×10^4, and 1.4×10^4 V/m for the position of the POPL at 1.0 × Dph, 2.0 × Dph and 4.0 × Dph from the right phase, respectively.

Figure 7 shows the electric field of 220 kV using shield wires which is decreased from 1.7×10^4 V/m (without using shield wires) when the POPL is exactly under the right phase of the TL with height of phase (H_{ph}) at 10 m above the ground level to 1.25×10^4 V/m (with using shield wires), and 1.0×10^4, 0.7×10^4, 0.5×10^4 and 0.4×10^4 V/m with H_{ph} at 15, 20, 25, and 30 m, respectively.

Figure 7 exhibits the results of the calculation of the electric field at the height of one meter over the ground without using the shield wires under the stressed wires (220-kV EHVACTLs) at the height of 75% of the tower height H. It is quite clear that using the shield wires under the 220-kV EHVACTLs reduces the concentration of the electric field at the oil 'pipelines' surface, and its shape is more uniform if the position of the parallel oil pipelines is exactly under the right phase of the TL or at 1.0, 2.0, or 4.0 × Dph from the right phase of the TL, as shown in Figure 7A, B, C, and D, respectively. The shield wires are affected by decreasing the concentration of electric field under the EHVACTLs and on the surface of the parallel oil pipelines.

Figure 8 shows the results of the calculation of the electric field using the shield wires at the level of oil pipelines (at the height of one meter over the ground) under the 220-kV EHVACTLs with the position of the parallel oil pipelines at 2.0 × Dph from the right phase of the TL at the height of 75%, 50%, and 25% of the tower height H. With increasing the distance between the ground shield wires and the

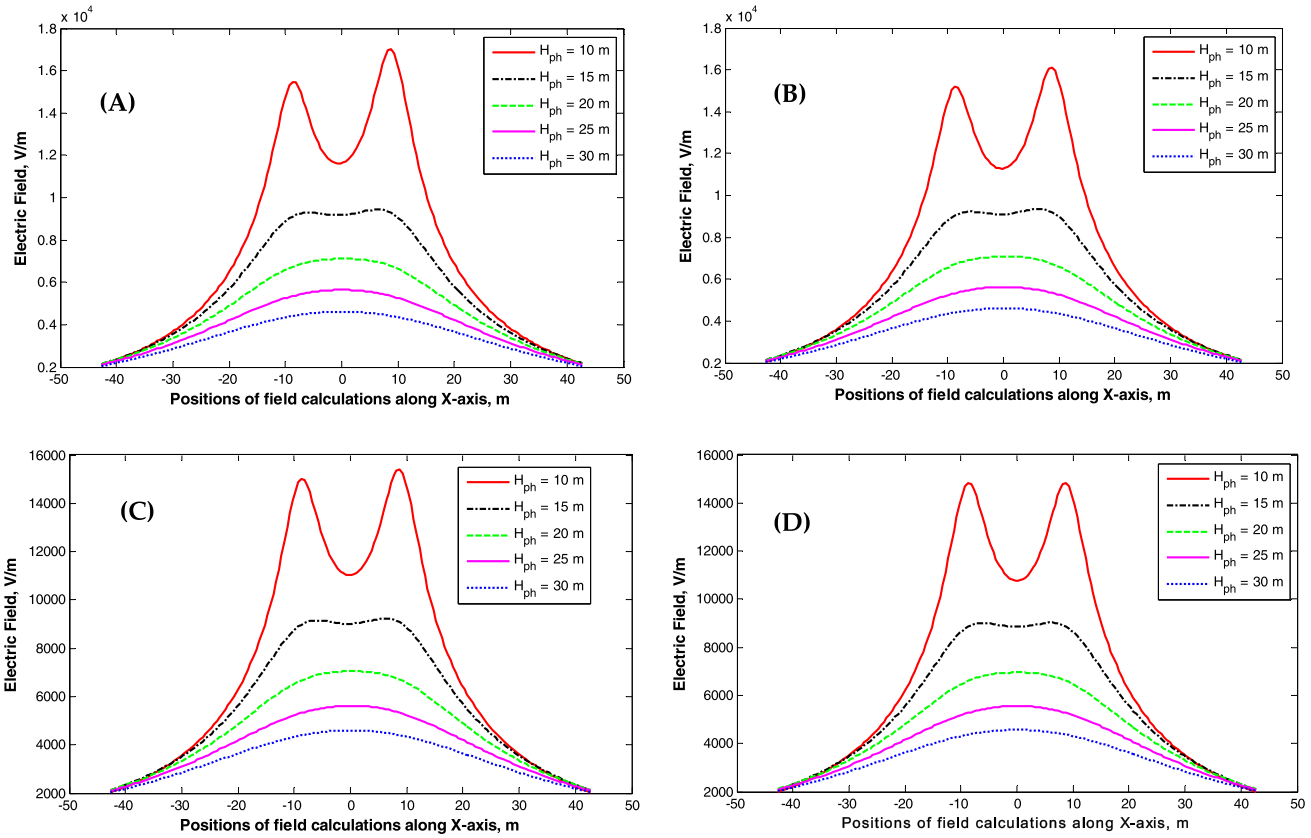

Fig. 6 Calculation of the electric field at a height of one meter over the ground at the same parallel oil pipelines level under the 220-kV EHVACTLs without using shield wires with the position of the parallel oil pipelines is **A** exactly under the right phase of the TL, **B** at 1.0 × Dph from the right phase of the TL, **C** at 2.0 × Dph from the right phase of the TL, and (**D**) at 4.0 × Dph from the right phase of the TL

stressed wires, the electric field on the level of oil pipelines is decreased, as shown in Figure 8A, B, and C, respectively.

3.4 Discussion of results at 220-kV EHVACTLs with parallel oil pipelines

It is clear from Figure 6A through D that there is the significant effect of the position of POPL under the stressed 220-kV EHVACTLs without using shield wires. The concentration of the electric field is diminished from 1.7×10^4 V/m when the POPL is exactly under the right phase of the TL with height of phase10 m above the ground level to 1.6×10^4, 1.55×10^4, and 1.4×10^4 V/m at the position of 1.0 × Dph, 2.0 × Dph and 4.0 × Dph for the POPL at the right phase, respectively. This corresponds to 9.9, 8.8, and 17.6 % reduction in electric field concentration at positions of 1.0 × Dph, 2.0 × Dph and 4.0 × Dph for the POPL at the right phase, respectively. According to the previous discussion and obtained results in Figure 6, it is recommended to keep the POPL as far as possible from the EHVACTLs to achieve the minimal concentration of electric field on the POPL.

The effect of using shield wires as well as changing the position of the POPL under the stressed EHVACTLs as proposed in the second technique is demonstrated in Figure 7. The concentration of the electric field on POPL using shield wires under the EHVACTLs is reduced to suitable values and did not affect by the position of the POPL under or near the EHVACTLs as shown in Figure 7-A through D. The electric field concentration is mitigated from 1.75×10^4 V/m without using shield wires to 1.28×10^4 after using the shield wires. This corresponds to 26.9% reduction in field concentration as depicted in Figures 6 and 7, respectively. This concludes that the shield wires protect the POPL from the effect of electric field concentration as well as make it possible to keep the POPL everywhere under the stressed EHVACTLs.

The significant effect of distance between the ground shield wires and the stresses wires is addressed in Figure 8A, B, and C. With increasing the distance between the ground shield wires and the stressed wires via changing the height of the shield wires (H_{sh}), the electric field on the level of POPL is decreased as depicted in Figure 8A, B, and C, respectively. The concentration of the electric field at the shield wires (H_{sh}) height 75%, 50%, and 25 % of the tower height is decreased

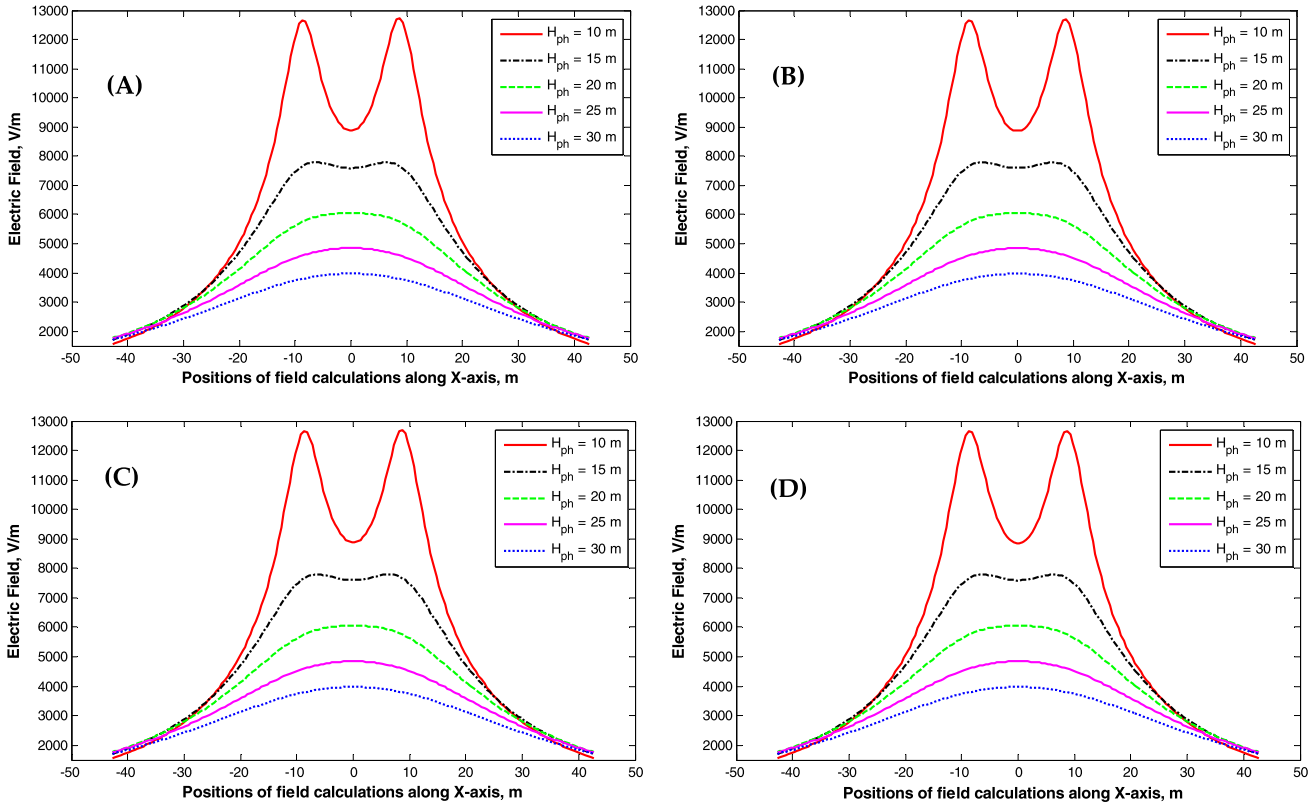

Fig. 7 Calculation of the electric field at a height of one meter over the ground at the same parallel oil pipelines level under the 220-kV EHVACTLs with using the shield wires at the height of 75% of the tower height H with the position of the parallel oil pipelines is **A** exactly under the right phase of the TL, **B** at 1.0 × Dph from the right phase of the TL, **C** at 2.0 × Dph from the right phase of the TL, and (**D**) at 4.0 × Dph from the right phase of the TL

to 1.28×10^4, 1×10^4, and 0.98×10^4 V/m with height of phase (H_{ph}) at 10 m above the ground level as depicted in Figure 8A, B, and C, respectively. This corresponds to 26.9, 42.9, and 44% reduction on electric field concentration as compared to the value of electric field without shield wires ($= 1.75 \times 10^4$ V/m).

4 Conclusion

The conclusions from this work can be summarized as follows: The electric field under the EHVACTLs is calculated using the well-known charge simulation method technique, especially its concentrations on the parallel oil pipelines. Two cases are studied in this study: The first case is 500 kV and the second is 220-kV AC transmission line. To mitigate or eliminate the electric field beneath the extra-high-voltage AC transmission lines (EHVACTLs), should use the shield wires under the stressed conductors or increase the distance between the towers and the parallel oil pipelines. Using the shield wires under the EHVACTLs will reduce/mitigate the concentration of the electric field on the POPLs by 17.65% and 24.71% if the POPL is precisely under the right stressed conductor of 500 kV and 220 kV, respectively. Besides, 20% and 21% concentrations are achieved if the POPL is at a distance from the right stressed conductor equal to the horizontal clearance between conductors of 500 kV and 220 kV, respectively. The results of the first technique revealed that with increasing the tower height from 10 m to 15, 20, 25, and 30 m, the electric field decreased by 43.75%, 62.5%, 68.75%, and 75%, respectively. Herein, employing the second technique, the electric field intensity is reduced by 20% and 21% depending on the POPL is placed at a distance from the right stressed conductor equal to the horizontal clearance between conductors of 500 kV and 220 kV, respectively. Besides, the results of third technique proved that the shield wires under the EHVACTLs reduced the electric field intensity on the POPLs by 17.65% and 24.71% for 500-kV and 220-kV TLs, respectively. Moreover, the electric field concentration was reduced by increasing the distance between the stressed conductors and shield wires. The shape of the electric field under the stressed wires is more uniform when the shield wires are utilized. The electric field under the EHVACTLs is mitigated by increasing the towers' height.

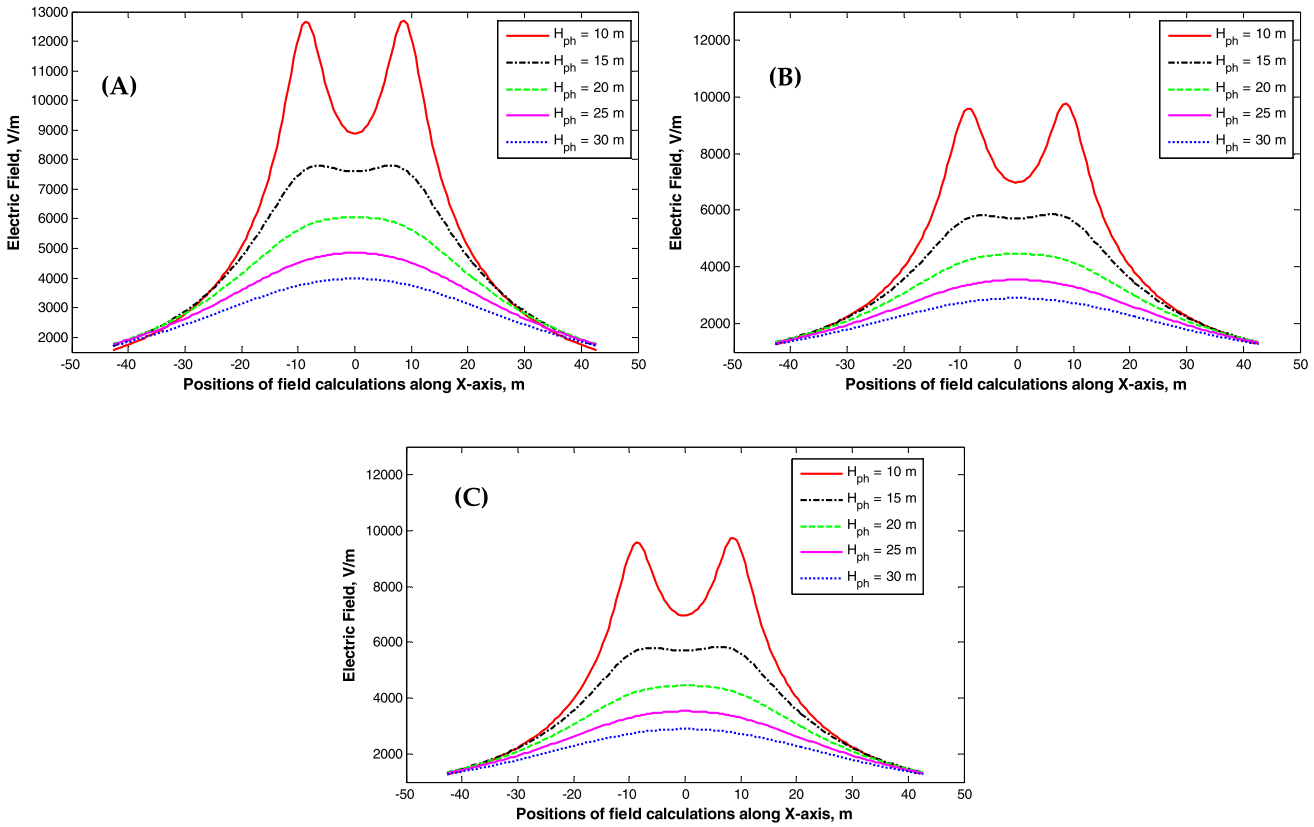

Fig. 8 Calculation of the electric field at a height of one meter over the ground at the same parallel oil pipelines level under the 220-kV EHVACTLs with using the shield wires with the position of the parallel oil pipelines is at 2.0 × Dph from the right phase of the TL at height of: **A** 75% of the tower height H, **B** 50% of the tower height H, and (**C**) 25% of the tower height H

This work's weakness is that it does not support research with experimental laboratory and/or actual field measurements due to safety requirements. Consequently, the authors urge that future work include real measurements to confirm the mathematical calculation findings acquired in this study through the experimental results.

Author contributions A.E, H.A.Z, and M. Abdelsattar wrote the main manuscript text. M.A prepared and drew all figures. A. Elnozahy wrote the literature review and introduction. H.A.Z did the simulation work. All authors reviewed and revised the manuscript.

Funding Open access funding provided by The Science, Technology & Innovation Funding Authority (STDF) in cooperation with The Egyptian Knowledge Bank (EKB). The funding was provided by the Science, Technology & Innovation Funding Authority (STDF) in cooperation with the Egyptian Knowledge Bank (EKB).

Data availability All data generated or analyzed during this study are included in this published article.

Declarations

Conflict of interest The authors declare no competing interests.

References

1. Shwehdi MH, Johar UM (2003) Transmission line EMF interference with buried pipeline: essential & cautions. In: International conference on non-ionizing radiation UNITEN (ICNIR), Electromagnetic Fields Our Heal, pp 1–13, 20–22 October 2003
2. Abdel-Salam M, Ziedan HA, Hossam-Eldin AA (2014) Induced voltages on nearby pipelines by AC Power lines. In: CIGRE Conference, Paris, France (i): 1–9
3. Radwan RM, Mahdy AM, Abdel-Salam M, Samy MM (2013) Electric field mitigation under extra high voltage power lines. IEEE Trans Dielectr Electr Insulation 20(1):54–62. https://doi.org/10.1109/TDEI.2013.6451341

4. Ismail H (2007) Effect of oil pipelines existing in an HVTL corridor on the electric-field distribution. IEEE Trans Power Deliv 22(4):2466–2472. https://doi.org/10.1109/TPWRD.2007.905368
5. Abdel-Salam M, Al-Shehri A (1994) Induced voltages on fence wires and pipelines by ac power transmission lines. IEEE Trans Ind Appl. https://doi.org/10.1109/28.287525
6. Ziedan HA, Alanazi MD (2018) Mitigation of electric fields/induced voltage on oil truck crossing EHVAC transmission lines; case study in Saudi Arabia. Int J Plasma Environ Sci Technol 12(1):7–11. https://doi.org/10.34343/ijpest.2018.12.01.007
7. Liu H, Li Q, Li H, Xue Z, Han M, Liu L (2021) Characteristics, and effects of electromagnetic interference from UHVDC and geomagnetic storms on buried pipelines. Int J Electr Power Energy Syst 125:106494. https://doi.org/10.1016/j.ijepes.2020.106494
8. Zhang B, Li L, Zhang Y, Wang J (2023) Study on the interference law of AC transmission lines on the cathodic protection potential of long-distance transmission pipelines. Magnetochemistry 9:75. https://doi.org/10.3390/magnetochemistry9030075
9. Thakur AK, Arya AK, Sharma P (2020) The science of alternating current-induced corrosion: a review of literature on pipeline corrosion induced due to high-voltage alternating current transmission pipelines. Corros Rev 38:463–472
10. Al-Gabalawy MA, Mostafa MA, Hamza AS, Hussien SA (2020) Modeling of the KOH-Polarization cells for mitigating the induced AC voltage in the metallic pipelines. Heliyon 6(3):e03417. https://doi.org/10.1016/j.heliyon.2020.e03417
11. Djekidel R, Bessedik SA, Spiteri P, Mahi D (2018) Passive mitigation for magnetic coupling between HV power line and aerial pipeline using PSO algorithms optimization. Electr Power Syst Res 165:18–26. https://doi.org/10.1016/j.epsr.2018.08.014
12. Popoli A, Cristofolini A, Sandrolini L (2020) A numerical model for the calculation of electromagnetic interference from power lines on nonparallel underground pipelines. Math Comput Simul 183:221–233. https://doi.org/10.1016/j.matcom.2020.02.015
13. Ouadah M, Touhami O, Ibtiouen R, Benlamnouar MF, Zergoug M (2017) Corrosive effects of the electromagnetic induction caused by the high voltage power lines on buried X70 steel pipelines. Int J Electr Power Energy Syst 91:34–41. https://doi.org/10.1016/j.ijepes.2017.03.005
14. Fotis G (2023) Electromagnetic fields radiated by electrostatic discharges: a review of the available approaches. Electronics 12:2577. https://doi.org/10.3390/Electronics12122577
15. Fotis GP, Ekonomou L, Maris TI, Liatsis P (2007) Development of an artificial neural network software tool for the assessment of the electromagnetic field radiating by electrostatic discharges. IET 1(5):261–269. https://doi.org/10.1049/iet-smt:20060137
16. Singer H, Steinbigler H, Weiss P (1974) A charge simulation method for the calculation of high voltage fields. IEEE Trans Power Appar Syst 93:1660–1668. https://doi.org/10.1109/TPAS.1974.293898
17. Ziedan HA, Mizuno A, Sayed A, Ahmed A (2010) Onset voltage of corona discharge in wire-duct electrostatic precipitators. Int J Plasma Environ Sci Technol 4(1):36–44. https://doi.org/10.34343/ijpest.2010.04.01.036
18. Popoli A, Sandrolini L, Cristofolini A (2019) Finite element analysis of mitigation measures for AC interference on buried pipelines. In: Proceedings of the 2019 IEEE international conference on environment and electrical engineering and 2019 IEEE industrial and commercial power systems Europe (EEEIC/I&CPS Europe), Genova, Italy, 11–14 June 2019
19. Wu X, Zhang H, Karady GG (2017) Transient analysis of inductive induced voltage between power line and nearby pipeline. Int J Electr Power Energy Syst 84:47–54
20. Abdel-Salam M, Mazen D. Transmission line electric field induction in humans as influenced by corona space charge. Available online at: http://cwl2004.powerwatch.org.uk/programme/posters/day3-abelsalem.pdf. Accessed 01 July 2020
21. Ziedan HA, Tlustý J, Mizuno A, Sayed A, Ahmed A (2010) Corona current-voltage characteristics in wire-duct electrostatic precipitators, Theory versus Experiment. Int J Plasma Environ Sci Technol 4(2):154–162. https://doi.org/10.34343/ijpest.2010.04.02.154
22. Ziedan HA, Rezk H, Al-Dhaifallah M, El-Zohri EH (2020) Finite element solution of the corona discharge of wire-duct electrostatic precipitators at high temperatures—numerical computation and experimental verification. Mathematics 8:1406. https://doi.org/10.3390/math8091406
23. Charalambous CA, Demetriou A, Lazari AL, Nikolaidis AI (2018) Effects of electromagnetic interference on underground Pipelines caused by the operation of high voltage A.C. traction systems: the impact of harmonics. IEEE Trans Power Deliv 33:2664–26721
24. Dushimimana G, Simiyu P, Ndayishimiye V, Niringiyimana E, Bikorimana S (2019) Induced electromagnetic field on underground metal pipelines running parallel to nearby high voltage AC power lines. In: E3S Web Conference 107:02004
25. El-Tamaly HH, Ziedan HA (2006) Sequence impedances of overhead transmission lines Carson's method versus Rudenberg's method. In: Published in conference proceedings of UPEC, 41st IEEE international universities power engineering conference, North Umbria University, Newcastle-Upon-Tyne, UK, pp. 298–302, 6th–8th September 2006. https://doi.org/10.1109/UPEC.2006.367763